



**JTI-CP-ENIAC-2011-1**

**DCC+G**

**DC Components and Grid**

STREP  
Contract Nr: 296108-2

**Deliverable: D 4.1.1**

**Detailed Specifications of Office Building  
Demonstrator**

Due date of deliverable: (03-31-2013)  
Actual submission date: (04-19-2013)

Start date of Project: 01 April 2012

Duration: 36 months

Responsible WP: Fraunhofer IISB

Revision: **accepted**

Dissemination level		
<b>PU</b>	Public	x
<b>PP</b>	Restricted to other programme participants (including the Commission Service	
<b>RE</b>	Restricted to a group specified by the consortium (including the Commission Services)	
<b>CO</b>	Confidential, only for members of the consortium (excluding the Commission Services)	

## 0 DOCUMENT INFO

### 0.1 Author

Author	Company	E-mail
Dr. Stefan Zeltner	Fraunhofer	<a href="mailto:stefan.zeltner@iisb.fraunhofer.de">stefan.zeltner@iisb.fraunhofer.de</a>
Leopold Ott	Fraunhofer	leopold.ott@iisb.fraunhofer.de

### 0.2 Documents history

Document version #	Date	Change
V0.1		Starting version, template
V0.2		Definition of ToC
V0.3		First complete draft
V0.4		Integrated version (send to WP members)
V0.5		Updated version (send PCP)
V0.6	4-4-2013	Updated version (send to project internal reviewers)
Sign off	4-18-2013	Signed off version (for approval to PMT members)
V1.0	4-19-2013	Approved Version to be submitted to EU

### 0.3 Document data

<b>Keywords</b>	
<b>Editor Address data</b>	Name: Leopold Ott Partner: Fraunhofer IISB Address: Schottkystr. 10 91058 Erlangen Germany Phone: +49 9131 761 363 Fax: E-mail: leopold.ott@iisb.fraunhofer.de
<b>Delivery date</b>	04-19-2013

### 0.4 Distribution list

Date	Issue	E-mailer
4-4-2013	V 0.6	<a href="mailto:al_dccg_all@natlab.research.philips.com">al_dccg_all@natlab.research.philips.com</a>
4-18-2013	Sign off	<a href="mailto:al_dccg_pmt@natlab.research.philips.com">al_dccg_pmt@natlab.research.philips.com</a>
4-19-2013	V 1.0	rolandweiss@siemens.com

## Table of Contents

<b>0</b>	<b>DOCUMENT INFO .....</b>	<b>2</b>
0.1	Author .....	2
0.2	Documents history .....	2
0.3	Document data.....	2
0.4	Distribution list .....	2
<b>1</b>	<b>INTRODUCTION.....</b>	<b>4</b>
<b>2</b>	<b>OFFICE TEST BED BUILDING .....</b>	<b>5</b>
<b>3</b>	<b>DC GRID ARCHITECTURE .....</b>	<b>7</b>
3.1	PHOTOVOLTAIC SYSTEM.....	8
3.2	DC DISTRIBUTION CABINET .....	10
3.3	CENTRAL RECTIFIER.....	12
3.4	BIDIRECTIONAL AC MAINS INTERFACE.....	12
3.5	MAXIMUM POWER POINT TRACKER .....	13
3.6	LIGHTING SYSTEM.....	15
3.7	POWER AND ENERGY METERING SYSTEM.....	19
3.8	24 V SUBGRID FOR IT APPLICATIONS.....	20
3.9	ADDITIONAL ENERGY SOURCES .....	23
3.9.1	MICRO-CHP UNIT .....	23
3.9.2	UHV SOLAR THERMAL COLLECTORS.....	24
<b>4</b>	<b>SUMMARY.....</b>	<b>26</b>
<b>5</b>	<b>REFERENCES.....</b>	<b>27</b>

---

## 1 Introduction

The European R&D project *Direct Current Components + Grid* (DCC+G) aims to develop innovative power semiconductors and products using them to increase the energy efficiency of commercial buildings. Hereby the partners of the project aim to contribute to the realization of the European Commission target that all new buildings in the EU shall be constructed as zero-energy buildings latest 2021 [1]. Examples of such buildings illustrate that electricity will replace fossil fuels in many energy related processes of such buildings [2]. Thus the cost effective and energy efficient use of electricity in buildings is an important area for technical innovations in the 21<sup>st</sup> century.

A 2-phase low voltage direct current (DC) grid with supply voltages of  $\pm 380 V_{DC}$  offers benefits compared with a 3-phase 400 V AC grid supply. Electricity from a DC supply can be controlled more flexible, with higher performance and efficiency, at lower cost than from AC electricity sources. For smaller power demands (e.g. in office buildings) a single phase 380  $V_{DC}$  grid is suggested.

The hard aims of the research and development project are to show that the use of direct current has advantages for certain loads compared to alternating current. This applies especially for the use of distributed regenerative energy generators like solar panels, local wind turbines and micro CHP units. Therefore, the goal is to show that the use of direct current reduces the whole power demand at 5 % while the cost for the use of solar electricity is reduced at 7 %.

For the feasibility test of the project, an office and a retail building were selected as experimental platforms. This is especially interesting, because the common electric loads in these types of buildings, e. g. lighting, HVAC and information technology, mostly need direct current. That means that the potential energy and cost savings through the cut out of two or more inverter stages are high.

This report describes the specification of the office building test bed. A part of the headquarter building of the Fraunhofer Institute of Integrated Systems and Device Technology (IISB) was selected as the "office test bed".

## 2 OFFICE TEST BED BUILDING

The Fraunhofer Institute for Integrated Systems and Device Technology (IISB) focuses on two big scientific areas. The first area is fundamental research in development and production of innovative semiconductor devices. The second area is the field of power electronics with special emphasis for automotive, energy storage and power distribution applications. Besides several laboratories, the institute runs its own clean room and in close cooperation an additional cleanroom with the department of electronic devices of the Friedrich-Alexander University of Erlangen and Nuremberg, which is the biggest scientific used cleanroom in Europe. **Figure 1** shows the institute's facilities.

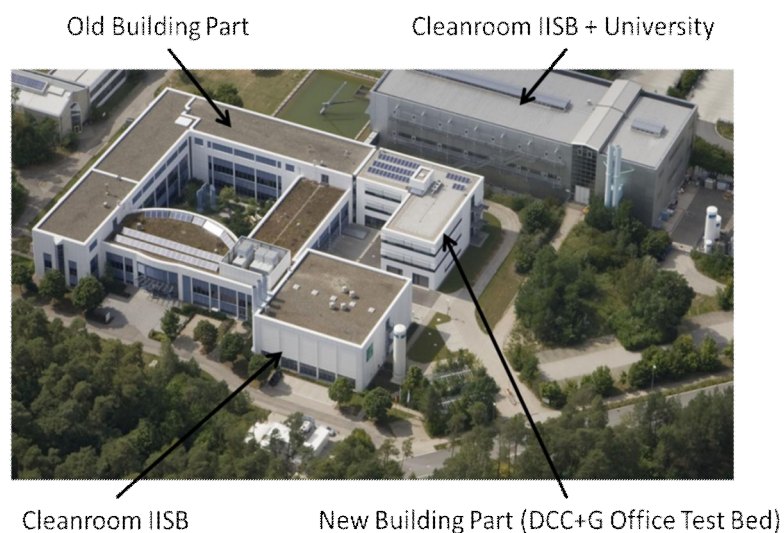


**Figure 1: Facilities of the Fraunhofer IISB in Erlangen**

For the DCC+G office test bed site, the second floor of the new building part of IISB (opened in March 2012), a combined office and laboratory building, was selected for several reasons. First, this building houses the power electronics division of the institute, which executes the work within DCC+G, and second, due to the fact that it is only about one year old, the entire electric infrastructure in this building part is well documented and modifications can be done more easily. Furthermore, a connection to the photovoltaic system on the roof can be easily done.

The electrical energy consumption of the whole facility lies at around 4 GWh per year, the demand for heat accounts for 2 GWh per year. Due to the high demand for cooling and filtered conditioned air in the production process of semiconductor devices, the HVAC (Heating Ventilation, Air Conditioning) applications are responsible for the biggest part of the energy consumption with a total percentage of around 64 %. The uninterruptable power supply (UPS) unit consists of a diesel generator and batteries. The diesel engine is kept in stand-by mode permanently to ensure a quick start-up time in case of an outage of the supplying grid. The batteries are designed to guarantee a hold-up time of time of 10 minutes for all security relevant applications like the server room. All in all, the uninterruptable power supply consumes 15 % of the whole electrical energy. Other major electrical energy consumers are entities to generate high pressurised air and vacuum with 6 % and the water treatment for cleanroom and laboratory processes with also 6 %. The remaining 9 % of the

institute’s electrical energy consumption is used mainly for lighting and information technology (IT) [3; 4]. **Figure 2** visualises the breakdown of the electrical energy consumption.

### Electrical Energy Consumption of Fraunhofer IISB

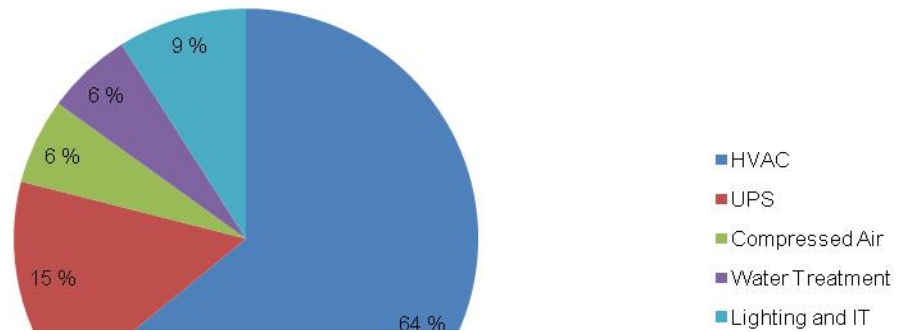


**Figure 2: Breakdown of major electric loads at Fraunhofer IISB**

Although HVAC and UPS applications account for more than two thirds of the electrical energy consumption of the IISB, they are not considered in the office test bed of the DCC+G project. Thus HVAC applications are planned for the retail building test bed, a possible scenario of a DC supplied cooling machines and ventilation could be deducted for the office test bed as well. Furthermore, IISB will investigate the inclusion of heat generating components that do not have a 380 V<sub>DC</sub> connection originally, like ultra-high vacuum solar thermal collectors. **Figure 3** shows the idea behind the DCC+G test beds including electrical and thermal system components.

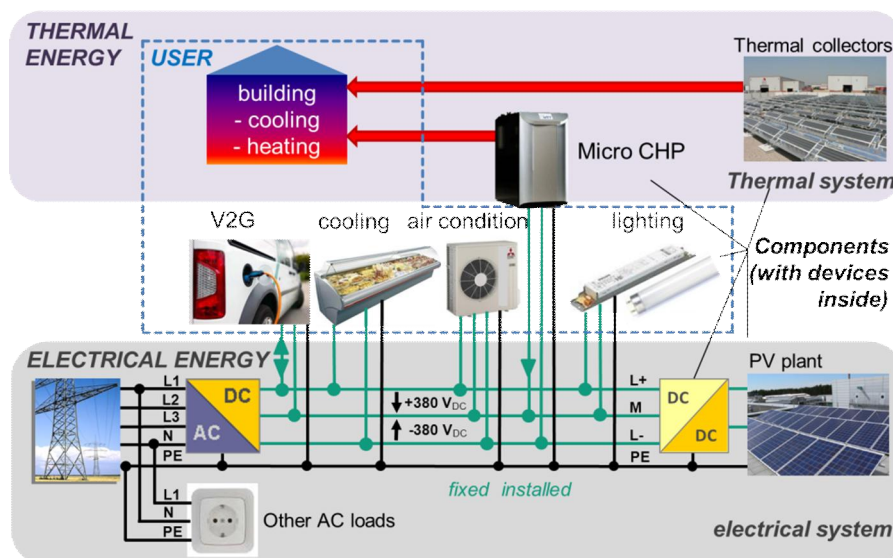


**Figure 3: Including thermal and electrical components within the office test bed**

### 3 DC GRID ARCHITECTURE

The office test bed will be arranged in the second floor of the new building. The floor consists of 12 offices for the scientific staff of the institute's power electronic department, one conference room, a small kitchen and a laboratory with a connection to the roof mounted photovoltaic system. The floor has its own sub-distribution unit for the AC grid supplying all electric loads, which basically consist of lights and IT applications. The whole lighting infrastructure contains 128 fluorescent lights with a total load of approximately 8 kW on a floor area of 1130 m<sup>2</sup>. Each room of the floor has two light bands for an equal distribution of light. To enable a proper comparison of AC and DC supplied lighting, one light band remains AC supplied, while the other one is modified for DC supply. Some of the IT equipment is modified to run with DC, so a resulting DC grid with a total load of approximately 5 kW can be set up on this floor. **Figure 4** depicts the setting of the test bed floor with exemplary pictures of different rooms.

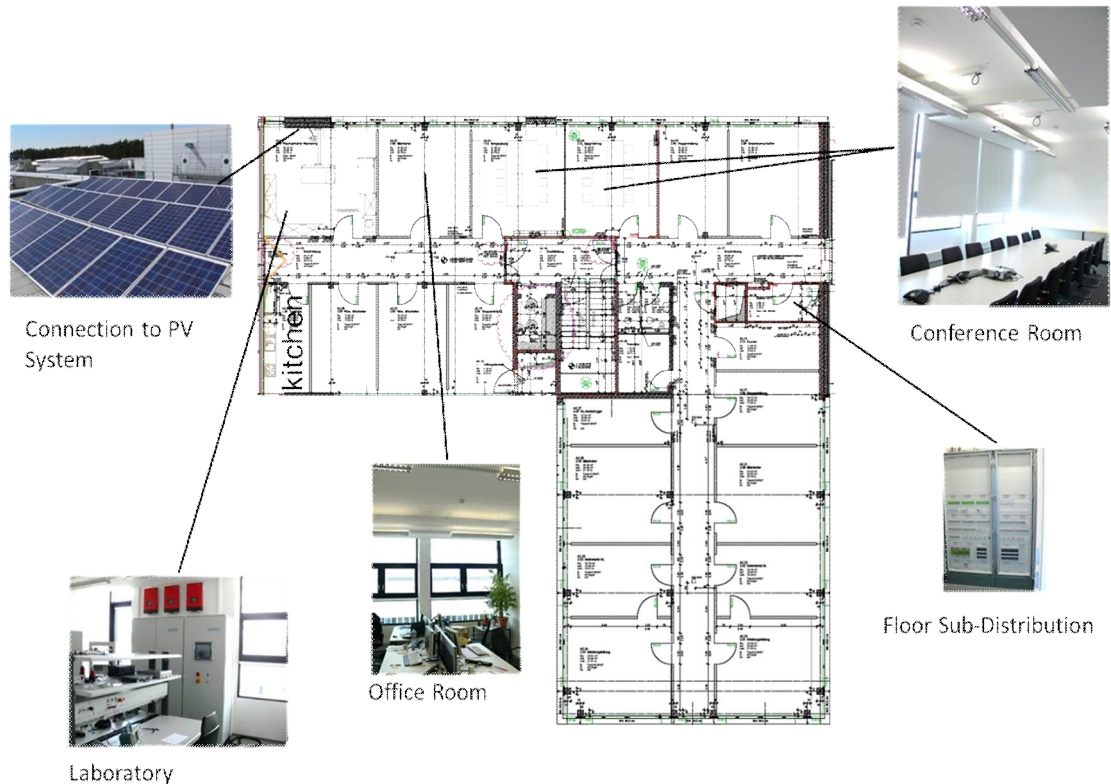


**Figure 4: Setting of office test bed floor**

A detailed description of all included components of the test bed can be found in the following sections.

### 3.1 PHOTOVOLTAIC SYSTEM

The system is mounted on the roof of the new building with a direct connection to the laboratory on the test bed floor. The entire system consists of three separate strings, each with its own inverter. The three inverters are located in the laboratory of the second floor and are needed to feed the energy generated by the three pv strings into the AC mains of the building. The specifications of the inverters from SMA are given in **Table 1**.

**Table 1: Technical data of solar inverter from SMA**

Technical data	Sunny Boy 3000HF
<b>Input (DC)</b>	
Max. DC power (@ $\cos\phi=1$ )	3150 W
Max. DC voltage	700 V
MPP voltage range	210 V – 560 V
DC nominal voltage	530 V
Min. DC voltage/start voltage	175 V/220 V
Max. input current/per string	15 A/15 A
Number of MPP trackers/strings per MPP tracker	1/2
<b>Output (AC)</b>	
AC nominal power (@230 V, 50 Hz)	3000 W
Max. AC apparent power	3000 VA
Nominal AC voltage; range	220, 230, 240 V; 180 – 280 V
AC grid frequency; range	50, 60 Hz; $\pm 4.5$ Hz
Max. output current	15 A
Power factor ( $\cos\phi$ )	1
Phase conductors/connection phases	1/1

In DC mode, these inverters are bypassed and the energy is fed directly over a DC/DC converter with integrated maximum power point (MPP) tracker. The converter is designed by Emerson Network Power. This allows a direct use of the pv-generated energy in the DC grid with higher conversion efficiency. **Figure 5** shows a close-up of the pv-system used in the office building test bed.



**Figure 5: Close-up view of office building test bed pv-system**

The panels of the pv-system consist of monocrystalline panels from the company SolarWorld, which have the following characteristic parameters for a solar irradiation of  $1000 \text{ W/m}^2$  and  $800 \text{ W/m}^2$  are documented in the following **Table 2**:

**Table 2: System parameters of SolarWorld SW 250 mono panel**

Parameter	STC ( $1000 \text{ W/m}^2$ , $25^\circ\text{C}$ )	NOCT ( $800 \text{ W/m}^2$ , $25^\circ\text{C}$ )
Maximum Power $P_{\max}$	$250 \text{ W}_p$	$183.3 \text{ W}_p$
Open-Circuit Voltage $U_{OC}$	$37.8 \text{ V}$	$34.6 \text{ V}$
Voltage at $P_{\max}$	$31.1 \text{ V}$	$28.5 \text{ V}$
Short-Circuit Current $I_{SC}$	$8.28 \text{ A}$	$6.68 \text{ A}$
Current at $P_{\max}$	$8.05 \text{ A}$	$6.44 \text{ A}$

The reason why either 12 or 14 panels can be connected in series per string is that in case of 14 panels in series the voltage at the point of maximum power would be around  $420 \text{ V}$  per string. This allows using a safe and simple, high efficient buck DC/DC converter as MPP tracker. In case of 12 panels connected in series the maximum power point voltage of the string is  $360 \text{ V}$  and requires therefore a boost DC/DC converter for MPP tracking and the connection to the HV DC bus.

The feed-in of the pv-system can be controlled via the DC distribution cabinet located in the laboratory of the office test-bed. To ensure a safe operation of the pv-system, a lightning and overload protection system was installed. The entire pv-system can be shut down via the so called “firefighter” switch located in the switch box of the system. For additional safety reasons a circuit to prevent back feeding of energy out of the DC system into the solar generator was included.

### 3.2 DC DISTRIBUTION CABINET

To control the flow of energy for the DC microgrid of the office test bed a DC distribution cabinet was designed containing a programmable logic controller (Beckhoff industry pc). The controller allows several different configurations of the system, which can all be monitored and analysed. The make-up of the DC distribution cabinet with its different input and output channels and connected applications can be seen in **Figure 6**.

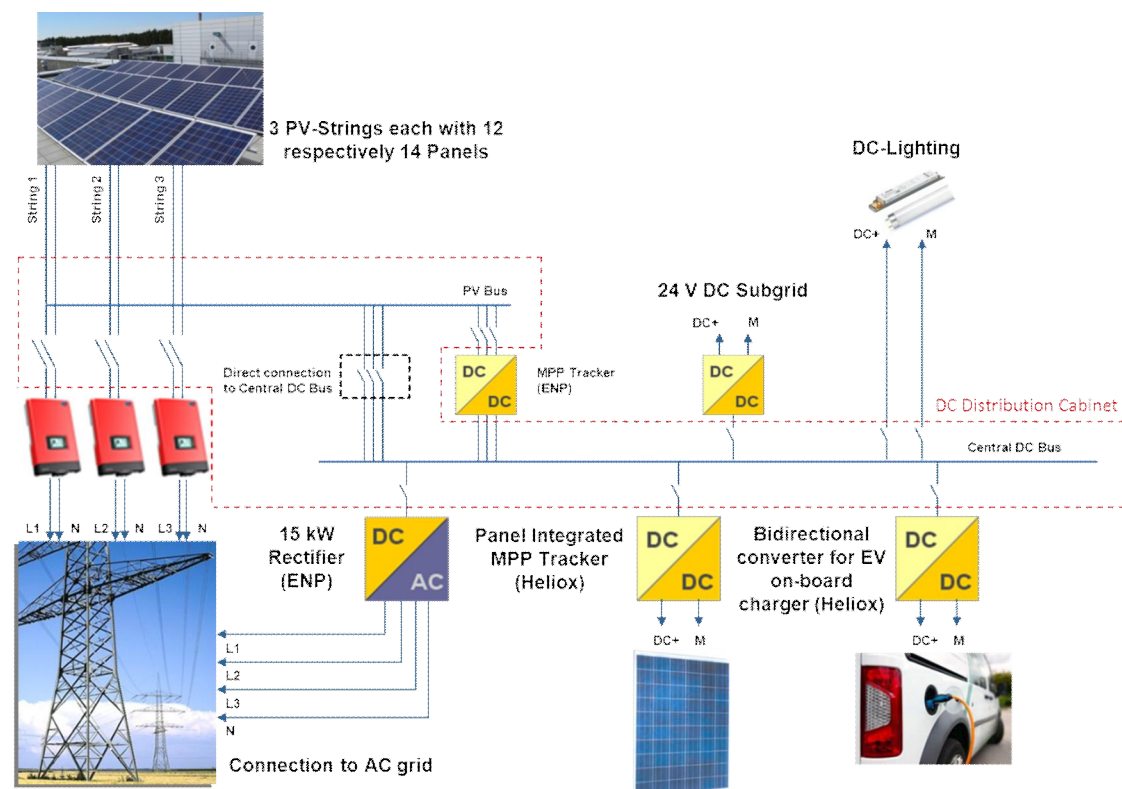


**Figure 6: Setting of DC distribution cabinet with connected appliances**

Each of the three strings of the office test bed can either be connected to the AC grid via the solar inverters or to the central DC bus. One can decide whether to connect a string directly to the central DC bus over a mechanical relay connection or using the maximum power point (MPP) tracker from Emerson Network Power (ENP). In the case that the pv-system voltage fits with the central DC voltage, this might influence the overall system efficiency and will be examined later in the test period of the office building demonstrator. Every DC grid application, like the central 15 kW rectifier, the panel integrated MPP tracker and electric vehicle (EV) charger, the DC lighting system and the converters for the 24 V<sub>DC</sub> subgrid, will be connected to the DC Bus via a suitable fuse for overcurrent protection. The DC distribution cabinet is designed for a maximum backbone current of 100 A and a maximum system voltage of 800 V<sub>DC</sub>. A pv-system voltage over 400 V<sub>DC</sub> can be reached by connecting two pv-strings in series, which is also possible over interconnections of a switching matrix. For the pv-strings themselves, three different configurations can be selected. The choice is between 12 or 14 panels per string or an automated switching between 12 and 14 panels per string. The control box can be divided in two different parts. One part contains all devices

needed to control the energy flow and the needed auxiliary AC voltage supply. One special requirement of the auxiliary AC voltage supply is that parts of it have to be buffered by capacitors or batteries to ensure a safe shut-down of the entire control box in case of an outage. Additionally, an insulation surveillance unit is included for protection against ground faults, in this case the whole DC system is operated galvanically isolated (so called IT network) from the AC grid. The picture of **Figure 7** depicts the functional groups of the DC distribution cabinet control box.

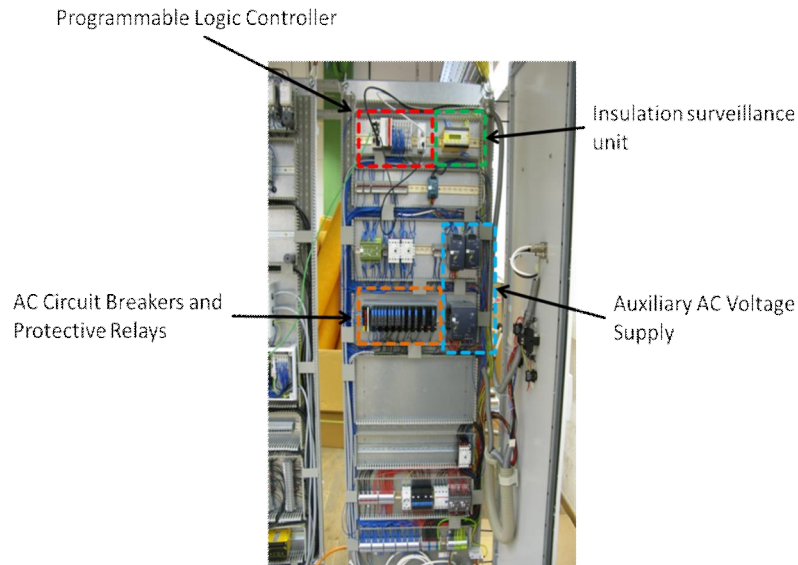


**Figure 7: Functional groups of the control system in the DC distribution cabinet**

The second part contains the controlled DC relays for the interconnection of the pv-strings with the external grid components like the inverters, the MPP tracker or a direct connection to the DC bus. To reduce the inrush currents and interrupting voltages for every connected application, pre- and discharge circuits were included for every feeder of the control box. These circuits are also used to shut-down the system voltage below a value of 60 V<sub>DC</sub> which is the maximum acceptable touch voltage. **Figure 8** gives an impression of the switching matrix in the control box. It has to be especially pointed out that each DC relay can only function in one certain direction of current flow due to the magnetic blow field mechanism used in the relays to extinguish the switch arc. So, to be able to switch off bidirectional flowing current, one needs two relays for each current path.



**Figure 8: Switching matrix of DC distribution cabinet**

An emergency stop system was designed to shut-down the system immediately under every possible fault condition.

### 3.3 CENTRAL RECTIFIER

The central rectifier with a power rating of 15 kW is provided by Emerson Network Power and establishes the connection of the LV DC grid of the office test bed to the three-phase AC grid. The rectifier enables a unidirectional power flow from the AC mains into the DC grid in case the generation inside the DC grid is not sufficient to meet the demand of the loads. The rectifier is also designed to provide active voltage droop control. The maximum output current of the rectifier is 45 A. The rectifier will be located in a 19 inch rack besides de DC distribution cabinet in the laboratory of the office building test bed. A picture of the rectifier can be found in **Figure 9**.



**Figure 9: 15 kW central rectifier module R400-1500e from Emerson Network Power [5]**

Detailed information of the central rectifier can be found in Deliverable D1.1.3 “Generic DC grid system specifications and architecture” [5]. In case the generation inside the DC grid exceeds the demand of the connected loads the generation needs to be derated to prevent the DC system voltage to exceed certain boundaries. Especially in cases a pv-system is used a bidirectional interface to the AC mains will make sense. So, the abundant energy can be fed back. The next section describes such an interface.

### 3.4 BIDIRECTIONAL AC MAINS INTERFACE

To enable a bidirectional energy flow between the low voltage DC grid and the AC mains, the laboratory of the office test bed possess an additional DC voltage source and a programmable electronic load that has the ability to feed electric energy back into the AC mains. **Figure 10** gives the basic setup.

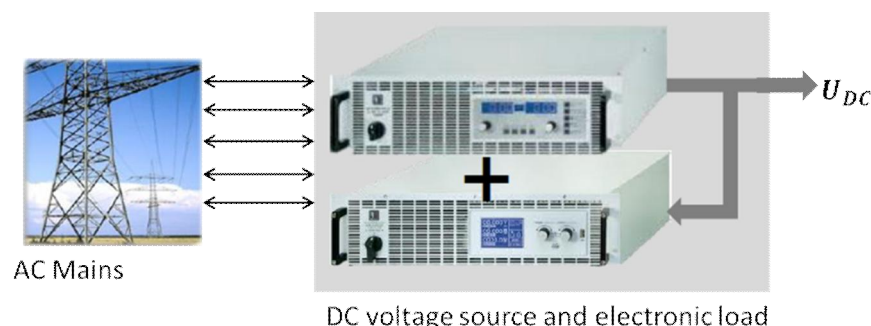


**Figure 10: Bidirectional AC/DC interface with DC source and programmable electronic load [6]**

This setup enables to build an experimental DC grid for arbitrary load profiles up to 10.5 kW and to evaluate the behaviour of the DC grid under dynamic load changes. Both, electronic load and DC source are embedded in a laboratory standard 19 inch rack. The so build up system can be easily cascaded upwards with additional

electronic loads to enable even higher power levels [6]. **Table 3** and **Table 4** give the basic data of the electronic load and the used DC power source.

**Table 3: Basic data of electronic load [6]**

<b>Electronic Load: EA-ELR 9000 10.5 kW</b>	
Input DC voltage range	0...500 V
Input DC current range	0...90 A
Input power range	0...10.5 kW
Average back feeding efficiency	93 %

**Table 4: Basic data of DC power source [6]**

<b>Voltage Source: EA-PS 8600-70</b>	
Output DC voltage range	0...500 V
Output DC current range	0...70 A
Output power range	0...15 kW

### 3.5 MAXIMUM POWER POINT TRACKER

To ensure the operation of the pv-system at its maximum power point a MPP tracker is integrated into the system. The tracker is basically a DC/DC converter interfacing the pv-strings with the HV DC bus. The applied control algorithm is especially edited for the characteristic curve of the pv-strings. The input current is controlled so that the panels operate in the point of maximum power matching the current irradiation. A good example for such a control algorithm is the so called “perturb and observe” (P&O) method, where the impact on the system of a small change in one of the system parameters is observed and it is then decided whether power output was increased by that change or not. This method is done continuously to reach an operating point near the current maximum power point of each pv-string. For a detailed description of the P&O and further MPP tracking algorithms see [5].

For the office test bed three different possibilities to connect the pv-strings to the central DC bus are examined. The first one is a central MPP tracker for all three strings connected in between the pv-string and the DC bus as seen in **Figure 11**.

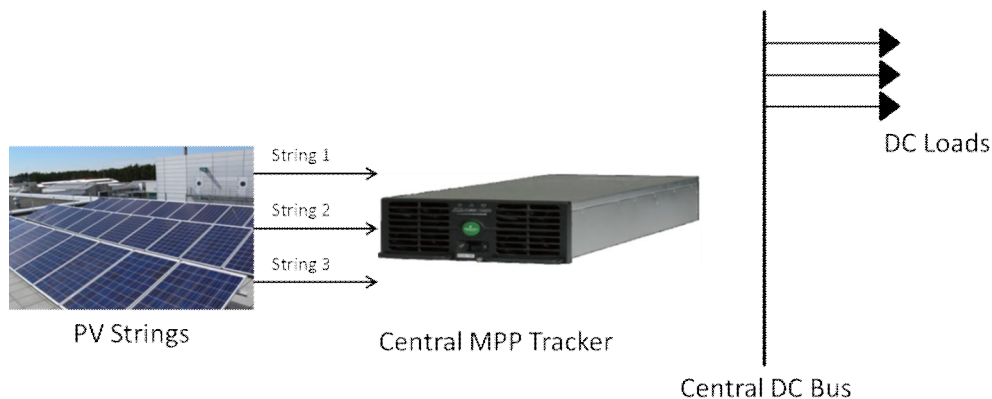


**Figure 11: Bus connection of pv-strings via central MPP trackers**

The central MPP tracker and the central unidirectional rectifier from Emerson Network Power will be delivered in a common 19 inch rack. **Figure 12** gives the setting of the power rack. For the office test bed, only a minimal configuration of the power rack will be used consisting of one 15 kW rectifier and one 15 kW MPPT converter for the pv-strings. Further MPPT converters or rectifiers are optional in dependence on a future enlargement of the pv-system. The central DC bus will be a single-phase 380 V<sub>DC</sub> system.

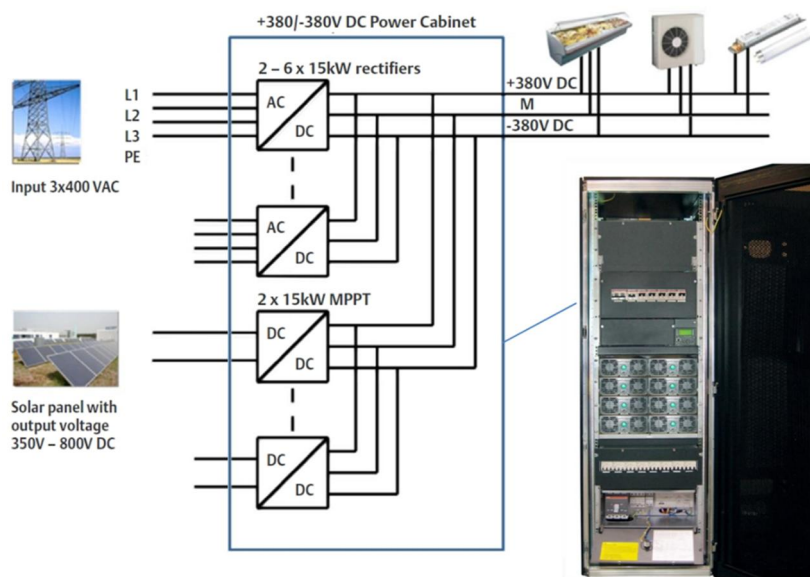


**Figure 12: Setting of Emerson Network DC power rack (example with a +/- 380 V DC grid)**

The second option will be supplied by the company Heliox with a panel integrated version of MPP trackers. This allows a better utilisation of each single panel. This is especially convenient to overcome partial clouding of the pv system and thus the efficiency and the energy output of every pv-string can be increased.

The third option is to connect the strings directly to the HV DC Bus. In this case the pv voltage must fit to the HV DC Bus voltage. It will be evaluated during the test period of the project if this configuration might have some benefits in terms of increased efficiency for the feed-in of solar generated energy.

All three connection options for the pv-strings can be selected over the touch screen control panel of the DC distribution cabinet.

### 3.6 LIGHTING SYSTEM

Since lights are one of the prevalent electrical energy consumers of office buildings, great emphasis will be put on these loads. The existing lighting infrastructure of the test bed building consists exclusively of T5 fluorescent lamps. Office, conference and the laboratory room are typically equipped with two light bands. Depending on the size of each room the light bands consist of one to four 98 W fluorescent tubes.

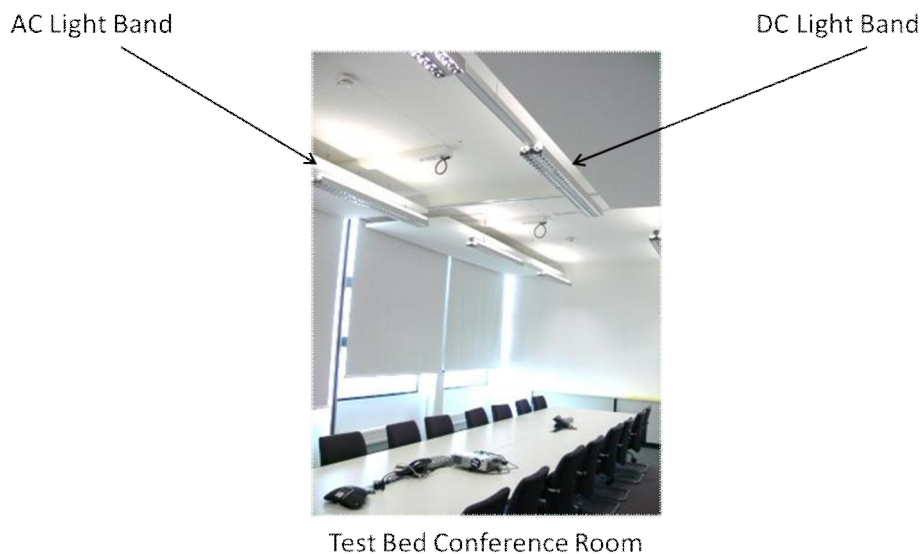


**Figure 13: Conference room equipped with two light bands**

As it will be explained in the section about energy measuring and monitoring, the idea is to maintain one light band with AC supply and rebuild the other light band in a room to function with DC supply. This approach enables an appropriate comparison between AC and DC fed tubes. Plus, it is possible to maintain at least one light band in each room in case the DC supply system is out of order. The measurement and interpretation of the results after the test period is simplified, because the efficiency of the energy conversion for the two different supplies of the fluorescent lights can be accurately done in the laboratory. The amount of saved energy can be computed out of the data from the AC measurement equipment (metering points will be explained in one of the following sections). All is needed is a detailed listing of the switching times for each single light band.

The switching of the light bands in the office building test bed is done via an EIB/KNX Instabus system. This system is a European standard for building automation. For the lighting system this means that the light switches of each room are connected to a relay unit. The relays and consequently the light bands are then switched on and off on behalf of the detected signals from each room. Of course, the used EIB/KNX Instabus mechanical AC relays are not able to switch on/off a DC voltage of 380 V without getting damaged. Therefore, a solid state relay circuit was designed which uses the AC output signal of the EIB/KNX relays to switch on/off the light bands. The basic setup of the switching procedure is shown in **Figure 14**.

The EIB/KNX Instabus controller can be accessed over Ethernet. The bus system is logging all switching actions of the lighting system. This eases the calculation of the efficiency gains through DC supply for lighting as it was already explained.

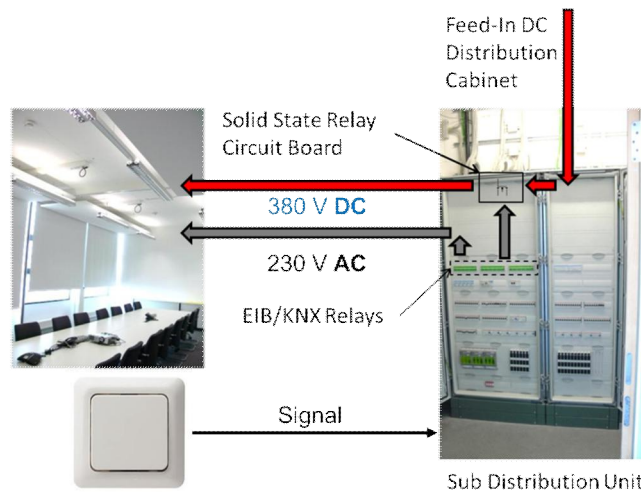


**Figure 14: On/off switching of AC and DC lights via EIB/KNX bus**

The circuitry to use the AC signal from the Instabus relays was designed under the premise that it should have a galvanic insulation between AC and DC side and of course to waste as less energy as possible. The result can be seen in **Figure 15**.

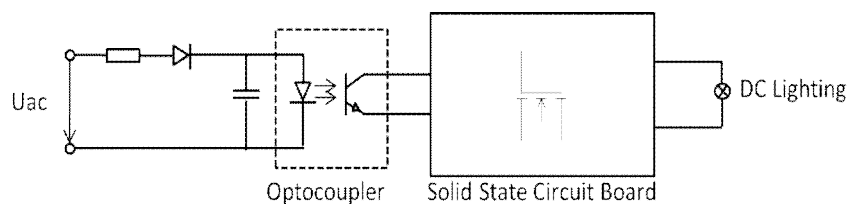


**Figure 15: Designed circuitry for the switching of the DC lights**

The AC signal is rectified and smoothed in the first place. The galvanic insulation is achieved via an optocoupler. The output of the optocoupler is used to switch on/off the driver circuit of an Infineon CoolMOS low-side switch.

To use the existing fluorescent T5 lamps in the offices with the DC supply, the control circuit of the lights can be simplified significantly in comparison with the AC case. **Figure 16** gives the makeup of the power supply unit in AC configuration.

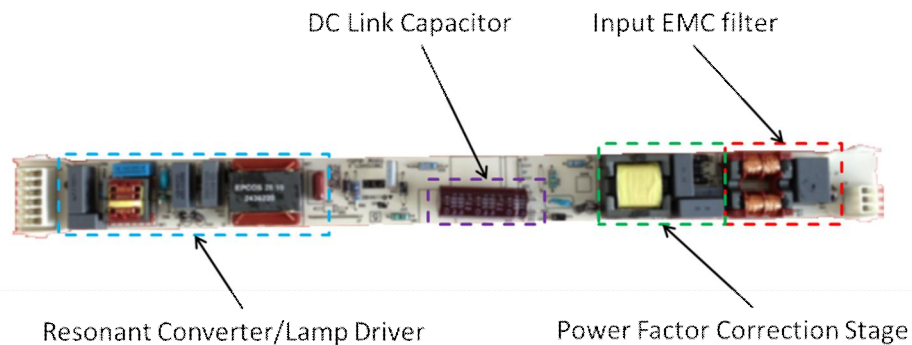


**Figure 16: Power supply unit of fluorescent Lamps in AC configuration**

For DC supply the Power Factor Correction (PFC) stage can be removed from the power supply unit. In the laboratory tests, the EMC filter was also removed, but it still needs to be verified whether this is also possible in regular grid operation. Additionally, the DC link capacitor can be reduced. One can see that the savings for electronic components can therefore reach a value of 50 %. In **Figure 17** the bread boarding of the modified control gear is depicted.

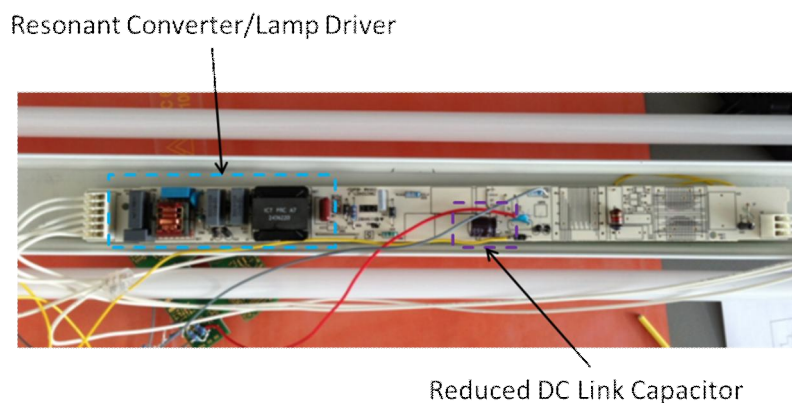


**Figure 17: Modified Control power supply unit for DC configuration**

The DCC+G office test bed will also provide a possibility to investigate LED lighting technology too. Therefore two floors of the old building part (see **Figure 18**) are selected for the installation of Philips LuxSpace LED downlight [7]. The floors in their current state with spot lights with compact fluorescent energy-saving lamps are sensed to be very dark by the employees, because the illuminance level on the ground of the floor is at an average 100 to 200 lux, whereas an illuminance level of 500 to 700 lux is more desirable. Through the use of efficient LED spot lights the illuminance level and the efficiency for the allocation of light will be increased.

Two different floors were selected again to enable an accurate comparison between DC and AC driven lamps.



Floor At IISB Old Building With Energy Saving Lights



Philips LED Light Spot

**Figure 18: Floor with fluorescent lighting at the old building part of Fraunhofer IISB and Philips LED downlight [7]**



### 3.8 24 V SUBGRID FOR IT APPLICATIONS

Because the average office room equipment almost entirely needs DC for operation, the existing 24 V<sub>DC</sub> nanogrid in one room of the test bed building is connected to the 380 V<sub>DC</sub> microgrid over a DC/DC converter integrated in the bottom tank of the office room besides the conventional AC supply. The make-up is depicted in **Figure 20**.

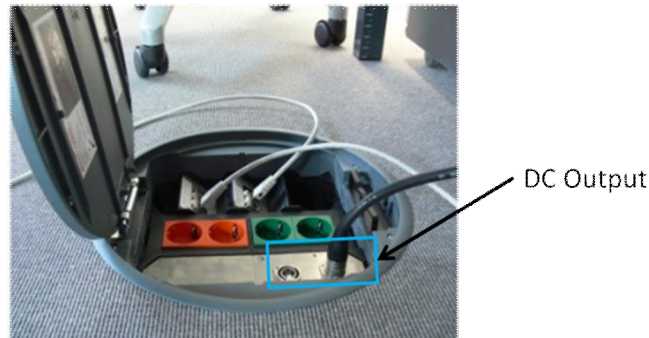


**Figure 20: Make-up of bottom tank for 24 V<sub>DC</sub> nanogrid**

The isolated DC/DC converter inside the bottom tanks is realised with two VI-modules from Vicor which are connected in series. The specifications of the two converters are as follows (**Table 5**):

**Table 5: Parameters of the isolated DC/DC converter to supply the 24 V DC nanogrid**

Model Number	B384F120T30
Input Voltage	360 – 400 V
Output Voltage	11.25 – 12.5 V
Output Power	300 W
Output Current	25 A

The basic circuitry with the two converters in series is shown in **Figure 21**. As it is explained in [9] the input circuitry of all devices connected to the HV DC grid is very important for a safe operation of the system in case of an occurring fault although it might reduce the overall efficiency. E. g. the input circuitry could consist of a diode for protection against inverse polarity protection and a fuse for protection against overcurrent. In this case, the input capacitances of the converters could be selected to overcome short-breaks of the system for around 10 ms.

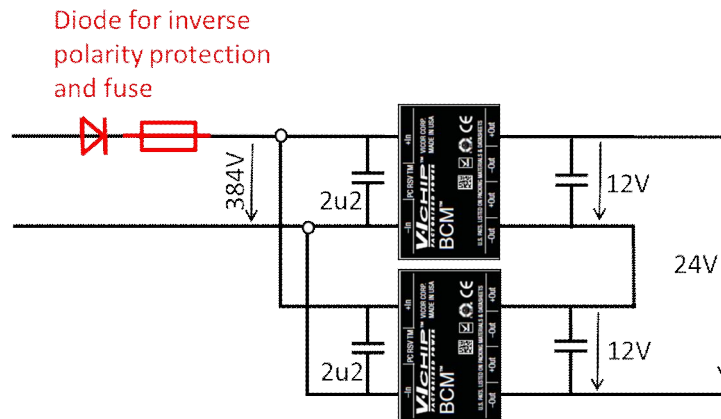


**Figure 21: Circuitry for 24 V<sub>DC</sub> nanogrid**

The biggest problem in realisation the 24 V<sub>DC</sub> nanogrid in the office room is the existence of a big variety of different input voltages for commercially available IT equipment. In case of the office test bed this means for example an input voltage of 14 V for the monitors and 20 V for the laptops and docking stations. So, the 24 V<sub>DC</sub> out of the isolated DC/DC converter need to be converted again (**Figure 22**).

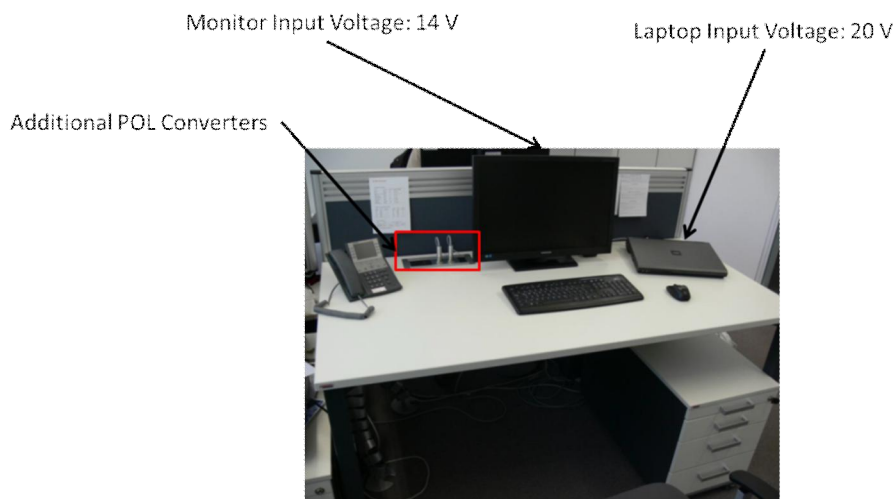


**Figure 22: Existing 24 V DC workplace at Fraunhofer IISB**

The different voltage levels for the IT equipment are provided by small point of load (POL) converters (**Figure 23**). These converters from Linear Technology are often used in IT equipment internally and have a very high efficiency over a wide operation range. The parameters of the converters can be found in **Table 1**.

**Table 6: Parameters of point of load (POL) DC/DC converter for IT loads**

Model Number	LTM8026
Input Voltage	6 – 36 V
Output Voltage	1.2 – 24 V
Output Power	Up to 120 W
Output Current	Up to 5 A

For the needed output power range of 30 to 40 W, the efficiency of the POL converters can be assumed to be around 95 % [13].

As can be seen, this significantly reduces the size of the power supply. Of course, this additional conversion stage lowers the overall efficiency. In the course of a possible standardisation of voltage levels for IT equipment with direct DC connection, this problem could be eliminated and the efficiency of the whole power supply can be increased.



Connector Plug Integrated POLs



Comparison of AC and DC Power Supply

**Figure 23: Allocation of different voltage levels for IT equipment**

### 3.9 ADDITIONAL ENERGY SOURCES

Besides the pv-system, the office test bed will provide an experimental platform for additional power sources, namely a micro CHP unit and ultra-high vacuum (UHV) solar thermal collectors. Since a connection to the existing heating system of the building is very expensive to establish, the considerations for this additional energy sources are focused mainly on the electric part. But using these techniques together with absorption cooling machine is highly interesting (but not a focus of the DCC+G project).

#### 3.9.1 MICRO-CHP UNIT

The proposed  $\mu$ -CHP unit can generate an electric power level of 3 kW and a thermal power level of 14.4 kW and is manufactured by Micro Turbine Technology (MTT) BV. In contrary to many  $\mu$ -CHP systems the solution of MTT uses a micro turbine instead of a combustion engine. The system uses the turbocharger technology which is well known from automotive applications. This solution promises great reliability, long lifetime and low maintenance costs. Natural Gas is used as fuel for the  $\mu$ -CHP unit.

The problem is that the Fraunhofer IISB building does not have a connection to the natural gas grid. This means that either a connection to the natural gas grid has to be established or a storage tank has to be used for the natural gas. Another idea is to use waste hydrogen gas that accumulates from time to time in cleanroom processes at the IISB mixed with natural gas. It still needs to be proven, if this is possible to achieve with the proposed  $\mu$ -CHP unit. The location of the  $\mu$ -CHP would be therefore selected to be as near to the cleanroom hydrogen output as possible.

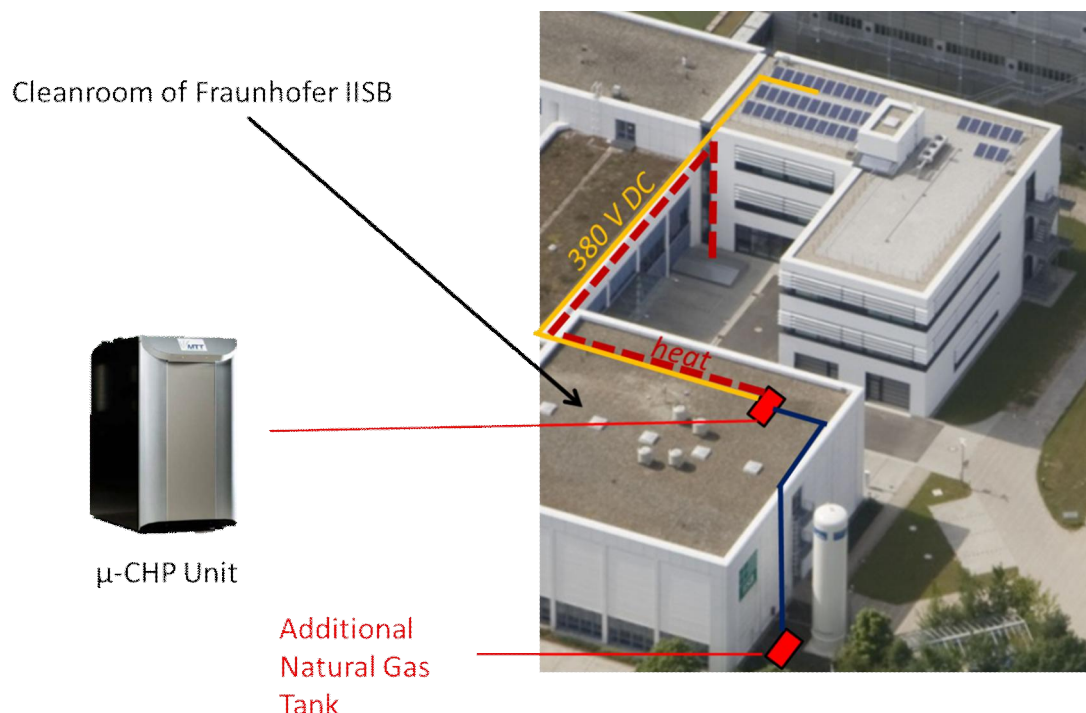


Figure 24: Possible location of  $\mu$ -CHP unit and connection to office test bed microgrid

**Figure 24** shows the possible locations of the  $\mu$ -CHP unit and both the electrical connection to the office test bed DC grid and a possible connection to the heating system of the building.

Principal statutory requirements are very strict for the installation of such a system, especially in a cleanroom environment. A large effort has to be done to fulfil fire protection requirements; e. g. the whole  $\mu$ -CHP installation will be embedded in a box that can prevent ignition for at least 90 minutes. This also applies for all other components of the system like the gas supply pipes and the ventilation.

### 3.9.2 UHV SOLAR THERMAL COLLECTORS

The UHV solar thermal collectors will be provided by the company SolCalor. The techniques used in the solar thermal collectors to sustain the ultra-high vacuum inside the panel were derived from the technology transfer policy of CERN.

There are basically two ways to generate electricity out of the heat from the collectors. The first is to use the heat from the collectors to provide steam for a micro turbine. The second way is to use a thermal electric generator (TEG) to directly generate electricity out of difference of temperature between the hot solar fluid from the collectors and a heat sink. Clearly, the efficiency of the energy conversion in the second case is much lower ( $\eta \approx 6\%$ ), but due to the complexity of the realisation of a steam turbine process, the second option was selected. **Figure 25** shows the proposed installation.

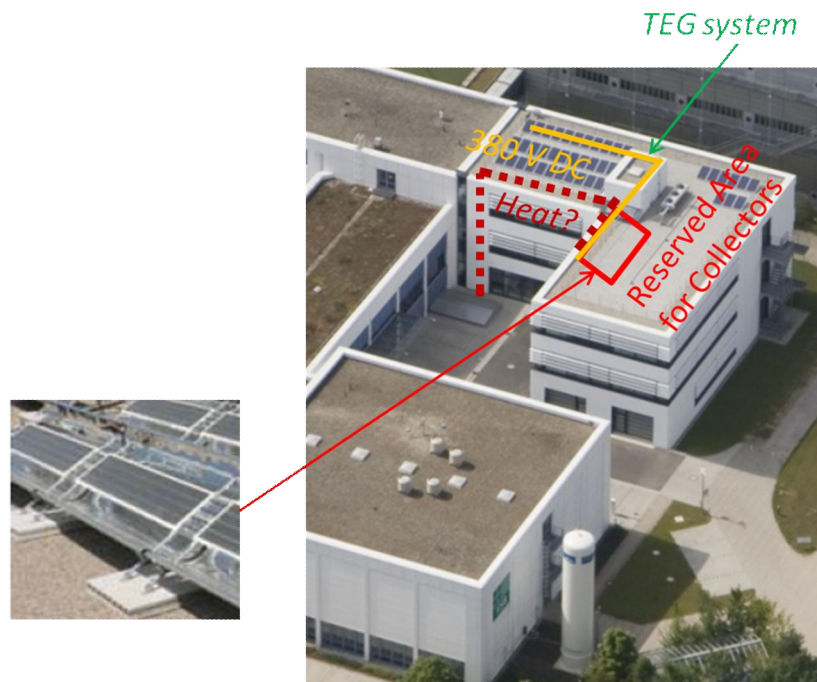


**Figure 25: Proposed solar thermal system for the office test bed**

The basic idea of this installation derives from [10]. In this work a new TEG system is designed for stagnation prevention in solar thermal systems. Stagnation occurs if the heat generation of the collectors exceeds the absorbing capability of the buffer storage. For this case special expansion vessels are included in the system to prevent the collectors from damage through the further expansion of the solar fluid. The thesis

proposes a bypass path for the solar fluid through a heat sink that contains the TEGs. This way, at least some energy can be produced in case of stagnation and the heat is not lost in the expansion vessel anymore.

In case of the solar-thermal system of the office test bed, a connection to the building heat system is difficult to establish. The focus of the proposed solar thermal system at the office test bed is therefore exclusively the generation of electricity with the TEG modules. The hot solar fluid of the collectors will be channelled through a dissipator unit to cool it down (**Figure 26**). Expansion vessels are yet necessary for safety reasons.

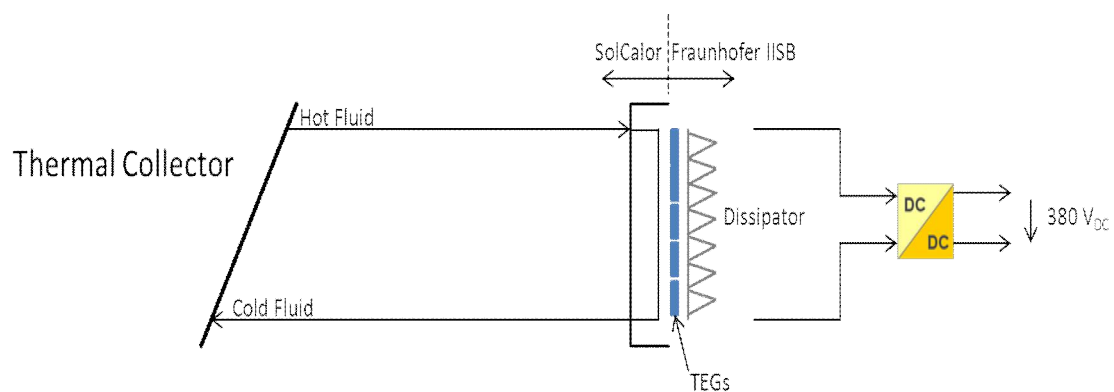


**Figure 26: Schematic to TEG module**

The TEGs are mounted between the hot solar fluid conducting pipes and the dissipator. The selected TEG modules [11] have their maximum power output if a temperature difference between hot and cold side of 125 °C ( $T_{\text{Hot}} = 175^{\circ}\text{C}$  and  $T_{\text{Cold}} = 25^{\circ}\text{C}$ ) is established. The number of the selected TEG modules that are connected in series depends on the desired output voltage. It is proposed to select a resulting operation voltage of the TEG system that lies below the 380 V<sub>DC</sub> of the HV DC Bus to use a simple boost converter topology for the DC/DC-converter. The number of collectors is then chosen in dependence of the thermal energy needed for the TEG modules to operate at their maximum output power level.

## 4 SUMMARY

The described office test bed at the Fraunhofer Institute for Integrated Systems and Device Technology provides a manifold foundation for all aspects of research in the field of DC microgrids.

The advantages of direct use of solar generated electricity can be shown through the pv-system belonging to the office test bed. Different connection possibilities of the pv-panels can be examined through the considerable possibilities the switching matrix of the DC distribution cabinet offers. Arbitrary load profiles can be examined through the DC lighting grid and the 24 V<sub>DC</sub> subgrid in connection with the electronic load. The designed DC distribution cabinet furthermore facilitates the connection of further grid components, like panel-integrated MPP trackers or a connection to an on-board charger for electric vehicles. Further energy sources, like  $\mu$ -CHP units and thermo electrical generators, can also be included in the system.

For an appropriate evaluation of the overall system performance, an energy metering system will be installed for detailed monitoring of the different energy flows. The office test bed fits consequently for the testing of almost all devices which are developed within the DCC+G project.

---

## 5 REFERENCES

1. European Commission: Energy Efficiency – Buildings, DIRECTIVE 2010/31/EU OF THE EUROPEAN PARLIAMENT AND OF THE COUNCIL of 19 May 2010 on the energy performance of buildings, [http://ec.europa.eu/energy/efficiency/buildings/buildings\\_en.htm](http://ec.europa.eu/energy/efficiency/buildings/buildings_en.htm)
2. K. Voss, E. Musall: Net zero energy buildings, ISBN 978-3-0346-0780-3, [http://shop.detail.de/eu\\_e/net-zero-energy-buildings.html](http://shop.detail.de/eu_e/net-zero-energy-buildings.html)
3. Manuel Mainka: Energieverbrauchsanalyse an einem Büro- und Laborgebäude im Rahmen der Optimierung des Qualitäts- und Umweltmanagementsystems einer wissenschaftlichen Einrichtung, Project Thesis, Friedrich-Alexander University Erlangen-Nurembourg, Department of Electronic Devices, 2010
4. Simon Linhardt: Energieanalyse-Bestandsaufnahme und Evaluierung von Einsparpotentialen am Beispiel eines Institutsgebäudes, Bachelor's Thesis, Friedrich-Alexander University Erlangen-Nurembourg, Department of Electronic Devices, 2011
5. ENIAC Project DCC+G Deliverable D 1.1.3 „Generic DC grid system specifications and architecture”, 2013
6. EA Elektro-Automatik GmbH & Co. KG: Product information ELR 9000 series, <http://www.elektroautomatik.de/products/electronicloads/elr9000.html>, 2013
7. Product information: Philips LuxSpace Compact High Efficacy LED, 2013
8. Product information: Siemens Multifunction Measurement Equipment SENTRON PAC, 2009
9. ENIAC Project DCC+G Deliverable 2.1.1 “State of the art DC grid technology, e. g. arc detection”, 2013
10. Ulland, Holger: Entwicklung von neuartigen thermoelektrischen Generatoren und ihr Einsatz in solarthermischen Anlagen, Doctoral thesis, University Duisburg-Essen, 2011
11. Data sheet: Thermoelectric Module QCG-127-2.0-1.3, Quick Cool Shop, 2012
12. Data sheet: LTM 8026 36 VIN, 5A CCC Step-Down  $\mu$ Module Regulator, 2013